Mechanical origin of power law scaling in fault zone rock

Charles G. Sammis, Geoffrey C. P. King

Mechanical origin of power law scaling in fault zone rock

Charles G. Sammis[1] and Geoffrey C. P. King[2]

Received 25 October 2006; revised 19 December 2006; accepted 4 January 2007; published 28 February 2007.

[1] A nearest neighbor fragmentation model, previously developed to explain observations of power law particle distributions in 3D with mass dimension $D_3 \approx 2.6$ ($D_2 \approx 2.6$ in 2D section) in low-strain fault gouge and breccia, is extended to the case of large strains to explain recent observations of $D_3 \approx 3.0$ ($D_2 \approx 2.0$ in 2D section) in the highly strained cores of many exhumed fault zones. At low strains, the elimination of same-sized nearest neighbors has been shown to produce a power law distribution which is characterized by a mass dimension near $D_3 \approx 2.6$. With increasing shear strain these isolated same-size neighbors can collide, in which case one of them fractures. The probability of two same size neighbors colliding and fragmenting in a simple shear flow is a function of the size and density of the two particles. Only for a power law distribution with $D_3 = 3.0$ is this collision probability independent of the size of the particles. **Citation:** Sammis, C. G., and G. C. P. King (2007), Mechanical origin of power law scaling in fault zone rock, *Geophys. Res. Lett.*, *34*, L04312, doi:10.1029/2006GL028548.

1. Introduction

[2] Faults that have large displacements are often modeled as a nested layered structure [*Chester and Logan*, 1986; *Chester et al.*, 1993, 2004; *Chester and Chester*, 1998]. At the center is a ''core'' comprised of a few centimeters of fine-grained ''cataclasite'' which appears to have accommodated most of the displacement. This cataclasite is usually cohesive, often has foliated flow structures and commonly contains narrow planar structures a few millimeters thick, which appear to be sites of further shear localization. *Chester et al.* [2005] have shown that the fragments within one such planar localization follow a power-law (fractal) distribution over a size range spanning nearly three orders of magnitude from 400 μm down to 60 nm. In 2-D section, they measured a mass dimension of $D_2 = 2.0$ (Figure 1). We use the term ''mass dimension'' to characterize the power law particle distributions rather than ''fractal dimension'', which is usually reserved for the Hausdorff dimension [see *Schroeder*, 1991]. The two measures are identical for simple geometrical fractals. Also, we use D_3 and D_2 to denote the mass dimension of particles imbedded in 3D and 2D respectively.

[3] The core is bordered by wider zones of fault gouge and breccia that can be meters thick with particle sizes ranging from microns to centimeters. The gouge and breccia is generally non-cohesive, usually shows no sign of significant shear strain, and also tends to have a power-law size distribution, but with a mass dimension closer to $D_2 = 1.6$ [*Sammis et al.*, 1987]. Particle distributions in cataclasite and gouge are compared in Figure 1.

[4] The gouge and breccia zones are bordered, in turn, by fractured (but not fragmented) wall rock in which the fracture density (damage) decreases to the regional background level over a distance on the order of 100 meters [*Chester and Logan*, 1986; *Wilson et al.*, 2003; *King and Sammis*, 1992]. There is a wide range of variation in this basic structure, particularly in the widths of the constitutive layers and in degree of symmetry about the core [*Ben-Zion and Sammis*, 2003; *Biegel and Sammis*, 2004].

[5] Field studies by *Chester et al.* [1993] and *Billi and Storti* [2004] have documented an increase in mass dimension within a single fault zone from a value near $D_3 = 2.6$ in the breccia and gouge to a value near $D_3 = 3.0$ in and near zones of shear localization (Figure 2). A similar increase in fractal dimension near shear localizations was also documented in detachment faults in Death Valley, CA, by *Hayman* [2006].

[6] To explain the self-similarity found in low strain gouge and breccia, *Sammis et al.* [1987] proposed a ''constrained comminution'' model in which the observed dimension $D_2 = 1.6$ is a direct consequence of a particle's fracture probability being controlled by the relative size of its nearest neighbors. This model differs from those that describe commercial crushing and milling operations in which a particle's fracture probability is determined by its distribution of starter flaws, usually assumed to be Poissonian, and which results in exponential particle distributions [*Prasher*, 1987]. These differences reflect the fact that the particles are free to move relative to each other in the commercial processes, but are tightly locked in place during compressive shear loading in a fault zone. Under compressive shear, stress is transmitted along grain bridges that rotate to produce dilatation and are continuously forming and failing to accommodate shear deformation (Figure 3). A grain bridge is weakest when it contains two adjacent particles the same size. Compressive point loading between two same-size particles produces internal tension causing one of them to fragment. This process begins at the largest (and hence weakest) particle size in the initial distribution and continues until no particle of any size has a same-sized nearest neighbor. The topological property of having no same-sized nearest neighbors at any scale is a characteristic of the Sierpinski carpet that has a mass dimension of $D_2 = 1.58$, close to $D_2 = 1.6$ observed in 2D sections of gouge. *Steacy and Sammis* [1991] showed that the systematic elimination of same-sized neighbors in a cellular automaton produces a random fractal with dimension near $D_2 = 1.6$. *Biegel et al.* [1989] used a double-shear friction apparatus to generate

[1]Department of Earth Sciences, University of Southern California, Los Angeles, California, USA.
[2]Laboratoire de Tectonique, Mecanique de la Lithosphere, Institut de Physique du Globe de Paris, Paris, France.

0094-8276/07/2006GL028548

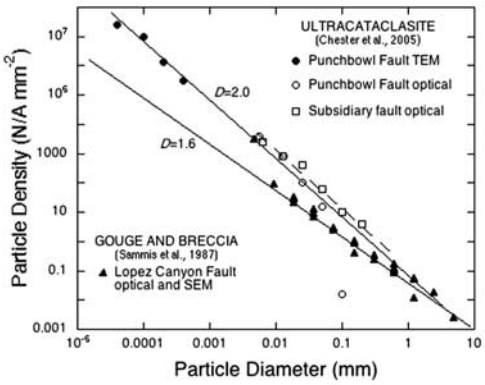

Figure 1. Comparison of the particle distribution in ultracataclasite with that in gouge and breccia. Note that both distributions are well described by a power law, but that the slope (fractal dimension) is larger for the ultracataclasite.

a power law gouge with $D_2 = 1.6$ in the laboratory. In these experiments, the evolution to a self-similar structure was observed to be associated with the transition from stable sliding to a stick-slip friction instability. A distribution with $D_2 = 1.6$ produces minimum dilatation in shear, which favors shear localization. Shear localization in gouge and breccia produces the highly-strained cataclasite core structure described above.

2. Nearest Neighbor Model for Fragmentation During Flow

[7] We now show how the simple ideas behind the constrained comminution model can be applied to a simple shear flow to explain the power law distribution with $D_2 = 2$ observed within highly strained fault cores. We begin with an analysis in 2D and then make a simple extension to 3D. In 2D, let $N_A(d)$ be the number of particles with diameter d per unit area. The average spacing between the centers of these particles is $\langle S(d)\rangle = \sqrt{N_A(d)}$ (Figure 4). If they are moving in a simple shear flow with strain rate $\dot{\varepsilon}$, then the average time between collisions is $\langle t(d)\rangle = \langle S(d)/v(d)\rangle$ where $v(d)$ is the relative velocity between two particles of diameter d that collide. The relative velocity of colliding particles of diameter d varies linearly between 0 for particles aligned in the shear flow to $v = \dot{\varepsilon}d$ for those that just touch in passing. The distance between the edges of two colliding particles also depends on their relative positions in the shear flow, varying between $S(d) - d$ for particles in line to $S(d)$ for those that just touch in passing. However, if each particle is involved in many collisions before it is fragmented, then the average distance over which is travels between collisions approaches $S(d)$ and the average time between collisions approaches $\langle t(d)\rangle \propto \langle S(d)/v(d)\rangle$, which may be written $\langle t(d)\rangle \propto (\dot{\varepsilon}d\sqrt{N_A(d)})^{-1}$. The average time between collisions per unit area of all size d particles is $\langle \bar{t}(d)\rangle \propto (\dot{\varepsilon}dN_A(d)\sqrt{N_A(d)})^{-1}$, and the frequency of collisions per unit area for size d particles is

$$\langle f(d)\rangle = \frac{1}{\langle \bar{t}(d)\rangle} \propto \dot{\varepsilon}d[N_A(d)]^{3/2} \qquad (1)$$

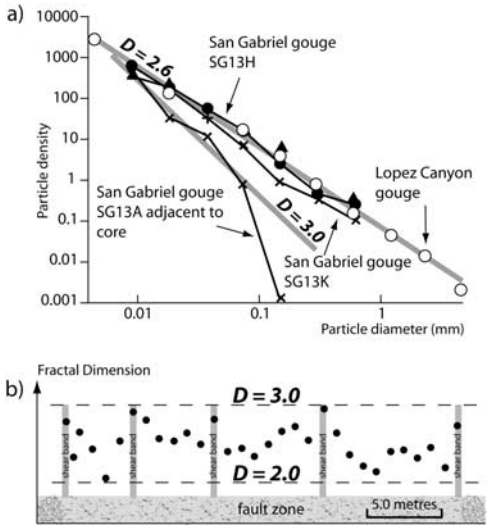

Figure 2. Fractal dimensions as a function of position in fault zones. (a) The increase in fractal dimension of fault gouge adjacent to the core of the San Gabriel Fault zone relative to the gouge and breccia at greater distances. Redrawn from *Chester et al.* [1993]. The distribution in the gouge and breccia from the Lopez Canyon fault from *Sammis et al.* [1987] is also shown for comparison. Note the fall-off in particle density for the larger particles in the sample adjacent to the fault core. This is an edge-effect produced by large strain and is discussed in the text. (b) An increase in fractal dimension in localized shear bands with the core of the Mattinata Fault in southern Italy. Redrawn from *Billi and Storti* [2004].

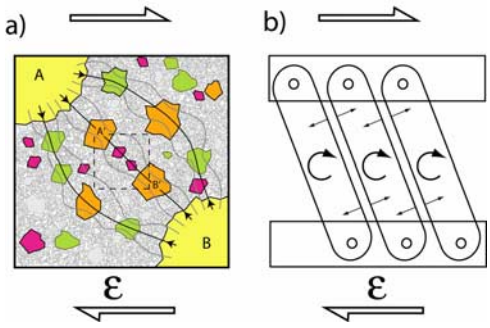

Figure 3. Low-strain fault gouge. (a) Stress paths. The stress between the largest particles shown (A and B in yellow) is transferred by a number of paths. Within the dashed square inset, the same geometry occurs at a smaller scale where the largest particles are now A′ and B′ in orange. This self-similarity can occur at successively smaller scales. (b) Grain bridges form when the material is strained. The increase in stress along the bridge causes particles to fracture in tension. The reduction in normal stress perpendicular to the bridges (associated with the rotation) further enables this tensile splitting. At any scale the tensile stress within a particle is greatest when in contact with a particle of similar size. Thus one of two adjacent particles of the same size is preferentially broken.

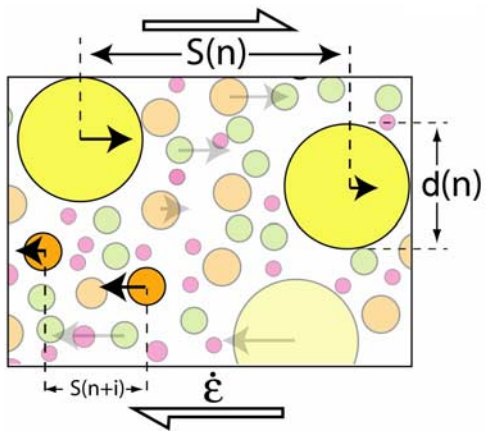

Figure 4. High strain fault gouge. For large strains, particles of the same dimensions that are isolated in the low-strain comminution can, as a result of flow, come into contact and cause one to fracture. Symbols in the figures are defined in the text.

The fraction of d-sized particles fragmented per unit time is

$$\langle F(d)\rangle = \frac{\langle \bar{f}(d)\rangle}{N_A(d)} \propto \dot{\varepsilon} d \sqrt{N_A(d)} \qquad (2)$$

For a fractal distribution of particles, $N_A(d) \propto d^{-D_2}$ and equation (2) can be written $\langle F(d)\rangle \propto \dot{\varepsilon} d^{\xi}$ where $\xi = 1 - D_2/2$. Note that if $D_2 = 2$, $\xi = 0$ and $\langle F(d)\rangle$ is independent of d. This means that if $D_2 = 2$ the number of particles in each class will be reduced by the same fraction in a given time increment and, if the new fragments are distributed among the smaller size classes in a scale-independent way, the distribution will remain at $D_2 = 2$. If $D_2 < 2$ then $\xi > 0$ and larger particles will be preferentially fractured increasing the dimension toward $D_2 = 2$. If $D_2 > 2$ then $\xi < 0$ and smaller particles will be preferentially fractured decreasing the dimension toward $D_2 = 2$.

[8] These scaling arguments also work for a 3D distribution of particles characterized by a volume distribution $N_V(d)$ and an average spacing of $\overline{S} = \sqrt[3]{N_V(d)}$. Since the simple shear flow is 2D, the average velocity between two particles of size d is again proportional to d and the average frequency of collision of all size d particles is $\langle f(d)\rangle \propto \dot{\varepsilon} d [N_V(d)]^{4/3}$. For a fractal distribution of particles, $N_V(d) \propto d^{-D_3}$ and $\langle F(d)\rangle \propto \dot{\varepsilon} d^{\xi}$. In this case $\xi = 1 - D_3/3$ so that if $D_3 = 3$, $\xi = 0$ and $\langle F(d)\rangle$ is independent of d. Hence, $D_3 = 3$ is the stable dimension for fragmentation during simple shear flow in 3D.

[9] The stability of $D_2 = 2$ in 2D can be illustrated by a simple computer automaton that operates on a discrete distribution in which the particles are grouped into classes n = 1, 2, 3, . . . where the size of a particle in class n is $d(n) = (1/2)^n$. At each time step, a random number generator chooses the class in which a particle is to be fractured based on the relative probabilities calculated using equation (1). The probability $P(n)$ that a class n particle will fracture in a time interval Δt is proportional to the frequency of collisions, and may be written $P(n) = P_o(\dot{\varepsilon}, \Delta t) d(n) [N_A(n)]^{3/2}$ in 2D. The number of particles in the chosen class is decreased by 1 while the number in the next smallest class is increased by 4 in order to conserve mass. The relative probabilities are then recalculated using the new values of $N_A(d)$ and the selection process is repeated.

[10] Figure 5 shows how the application of the automaton to an initial Sierpinski distribution ($D_2 = 1.58$) generates a stable distribution with $D_2 = 2$. Note that the there are fewer large particles in Figure 5 than expected for the fractal distribution. This is an edge effect that occurs because the largest particles are being fragmented but they are not being re-supplied by the fragmentation of particles larger than the upper fractal limit. A similar breakdown in self-similarity at large scales is often observed in real data (see Figure 2a).

[11] The evolution of a particle distribution toward $D_3 = 2.6$ at low strain and $D_3 = 3.0$ at high strain has been simulated in a 3D particle-based computer model by *Abe and Mair* [2005]. In their model, breakable bonds between individual particles allow the simulation of fracture during shear of large aggregate grains, each of which was initially composed of 8,000 individual particles.

3. Discussion and Conclusions

[12] In conclusion, observations of power law scaling of the particles in natural fault zones find different dimensions. For low-strain gouge a mass dimension of $D_3 = 2.6$ is observed while cataclasites that have been subject to larger shear strain exhibit a value close to $D_3 = 3.0$. If fragmentation is controlled by nearest neighbor particle interactions in which a particle is most likely to split when it encounters a particle of similar size, the two different mass dimensions can be simply explained. The measurement of mass dimension thus offers a way to distinguish regions that have been shattered at low strain from those that have been fragmented by significant shear.

[13] It may seem surprising that such a simple mechanism controls fragmentation, especially in the core of a fault where complex thermo-poro-elasto-dynamic processes are known to be important [see, e.g., *Rice*, 2006]. The impli-

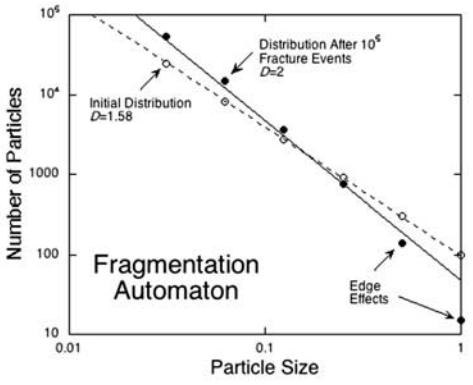

Figure 5. Evolution of an initial particle distribution having D = 1.58 into one having D = 2.0 using the fragmentation automaton described in the text. The deviation of large particles from the D = 2.0 line is an edge effect, since there are no particles being supplied at this end of the distribution from the fragmentation of still larger particles. Compare with the distribution in natural gouge adjacent to the core of the San Gabriel fault in Figure 2a.

cation is that the accommodation of strain by particle fragmentation is controlled by local geometrical constraints, and is largely independent of these additional complications. This argument is analogous to *King*'s [1983] explanation of the widely observed Guternberg-Richter scaling of earthquake magnitude with b = 1 in terms of local geometrical constraints of strain accommodation, independent of stress transfer, crustal fluids, and ductile relaxation also known to be important processes in regional seismicity.

References

Abe, S., and K. Mair (2005), Grain fracture in 3D numerical simulations of granular shear, *Geophys. Res. Lett.*, *32*, L05305, doi:10.1029/2004GL022123.

Ben-Zion, Y., and C. G. Sammis (2003), Characterization of fault zones, *Pure Appl. Geophys.*, *160*, 677–715.

Biegel, R. L., and C. G. Sammis (2004), Relating fault mechanics to fault zone structure, *Adv. Geophys.*, *47*, 65–111.

Biegel, R. L., C. G. Sammis, and J. H. Dieterich (1989), The frictional properties of a simulated gouge having a fractal particle distribution, *J. Struct. Geol.*, *11*, 827–846.

Billi, A., and F. Storti (2004), Fractal distribution of particle size in carbonate cataclastic rocks from the core of a regional strike-slip fault zone, *Tectonophysics*, *384*, 115–128.

Chester, F. M., and J. S. Chester (1998), Ultracataclasite structure and friction processes of the Punchbowl fault, San Andreas system, California, *Tectonophysics*, *295*, 199–221.

Chester, F. M., and J. M. Logan (1986), Implications for mechanical properties of brittle faults from observations of the Punchbowl fault zone, California, *Pure Appl. Geophys.*, *124*, 79–106.

Chester, F. M., J. P. Evans, and R. L. Biegel (1993), Internal structure and weakening mechanisms of the San Andreas fault, *J. Geophys. Res.*, *98*, 771–786.

Chester, F. M., J. S. Chester, D. L. Kirschner, S. E. Schulz, and J. P. Evans (2004), Structure of large-displacement strike-slip fault zones in the brittle continental crust, in *Rheology and Deformation in the Lithosphere at Continental Margins*, edited by G. Karner et al., pp. 223–260, Columbia Univ. Press, New York.

Chester, J. S., F. M. Chester, and A. K. Kronenberg (2005), Fracture surface energy of the Punchbowl fault, San Andreas system, *Nature*, *437*, 133–136.

Hayman, N. W. (2006), Shallow crustal fault rocks from the Black Mountain detachments, Death Valley, CA, *J. Struct. Geol.*, *28*, 1767–1784.

King, G. C. P. (1983), The accommodation of large strains in the upper lithosphere of the earth and other solids by self-similar fault systems: The geometrical origin of b-value, *Pure Appl. Geophys.*, *121*, 761–814.

King, G. C. P., and C. G. Sammis (1992), The mechanisms of finite brittle strain, *Pure Appl. Geophys.*, *138*, 611–640.

Prasher, C. (1987), *Crushing and Grinding Process Handbook*, John Wiley, Hoboken, N. J.

Rice, J. R. (2006), Heating and weakening of faults during earthquake slip, *J. Geophys. Res.*, *111*, B05311, doi:10.1029/2005JB004006.

Sammis, C. G., G. C. P. King, and R. Biegel (1987), The kinematics of gouge deformation, *Pure Appl. Geophys.*, *125*, 777–812.

Schroeder, M. R. (1991), *Fractals, Chaos, Power Laws: Minutes From an Infinite Paradise*, W. H. Freeman, New York.

Steacy, S. J., and C. G. Sammis (1991), An automaton for fractal patterns of fragmentation, *Nature*, *353*, 250–252.

Wilson, J. E., J. S. Chester, and F. M. Chester (2003), Microfracture analysis of fault growth and wear processes, Punchbowl fault, San Andreas system, California, *J. Struct. Geol.*, *25*, 1855–1873.

G. C. P. King, Laboratoire de Tectonique, Mecanique de la Lithosphere, Institut de Physique du Globe de Paris, 4, place Jussieu, F-75252 Paris, France.

C. G. Sammis, Department of Earth Sciences, University of Southern California, Los Angeles, CA 90089-0740, USA. (sammis@usc.edu)